Penerbit Akademia Baru

CFD Letters

Journal homepage: www.akademiabaru.com/cfdl.html
ISSN: 2180-1363

Condition for Non-Oscillatory Solution for Scalar Convection-Dominated Equation

Open Access

Aslam Abdullah[1,*]

[1] Department of Aeronautical Engineering, Faculty of Mechanical and Manufacturing Engineering, Universiti Tun Hussein Onn Malaysia, 86400 Parit Raja, Johor, Malaysia

ARTICLE INFO

Article history:
Received 19 February 2020
Received in revised form 16 April 2020
Accepted 21 April 2020
Available online 28 April 2020

ABSTRACT

The scalar convection-dominated flows are found in different science and designing applications which incorporates those concerning the computational fluid dynamics problems of mesh structure in the numerical estimations. These flows are thus essential in nature. Despite the fact that these types of flow have been widely discussed among fluid dynamists, the contribution of mesh and flow parameters in predicting spurious-oscillation free solutions remains unclear. In this research, the significance of the connections between the mesh structure and the scalar convection-dominated flow parameters is accentuated. A systematic technique is applied in the setting of the parameters of interest. In particular, we present the a priori formulation of condition to avoid spurious oscillatory solutions, which depends on both Peclet number as well as the number of grid. The condition is useful in a more efficient decision-making in the selection of the computational domain grid, and in eradicating some heuristic parts of the scalar concentration estimate. The results of the test case affirm the consistency of the condition. It is found that, given the right constant value in the amplification factor term within the spatial error growth model, the condition is able to capture the presence of kinks which mark the beginning of the oscillations.

Keywords:
Scalar convection-dominated flows; uniform grid; grid number; numerical oscillation

1. Introduction

Conservation equation in its generic form is given by

$$\partial_t(\rho\varphi) + \partial_{x_j}(\rho u_j \varphi) - \partial_{x_j}\left(\epsilon \partial_{x_j}\varphi\right) = s_\varphi, \tag{1}$$

where ρ is the density, φ is the conserved property, u_j are velocity components of the fluid in the axes directions at the point (x_1, x_2, x_3) at time t, ϵ is the diffusivity of φ, and s_φ is the source or sink of φ. We assume that $s_\varphi = 1$. Thus Eq. (1) is expressed as

* *Corresponding author.*
E-mail address: aslam@uthm.edu.my (Aslam Abdullah)

https://doi.org/10.37934/cfdl.12.4.2434

$$D_t(\rho\varphi) - \partial_{x_j}\left(\epsilon\partial_{x_j}\varphi\right) = 1 \tag{2}$$

This is scalar convection-dominated equation (SCDE). The substantial derivative in Eq. (2) is mathematically expressed by

$$D_t(\rho\varphi) = \partial_t(\rho\varphi) + \partial_{x_j}(\rho u_j\varphi) \tag{3}$$

Substituting Eq. (3) into Eq. (2) we have

$$\partial_t(\rho\varphi) + \partial_{x_j}(\rho u_j\varphi) - \partial_{x_j}\left(\epsilon\partial_{x_j}\varphi\right) = 1 \tag{4}$$

We can further simplify Eq. (4) into

$$\partial_t(\rho\varphi) - \partial_{x_j}\left(\epsilon\partial_{x_j}\varphi\right) = 1 \tag{5}$$

by assuming that the fluids are at rest, or the velocity is small $(u_j \approx 0)$, or diffusivity ϵ is large. The steady one-dimensional convection-diffusion problem reduces Eq. (4) into

$$\partial_x(\rho u\varphi) - \partial_x(\epsilon\partial_x\varphi) = 1 \tag{6}$$

involving the scalar whose concentration is denoted by φ. Details on these equations can be found in Ferziger *et al.,* [1]'s study. The abrupt growth of φ provides a severe test for computational methods, particularly in the selection of compatible grid structure over the computation domain.

We establish the relationship between the flow parameter of interest (i.e. the Peclet number Pe) in SCDE and the appropriate grid number N, by formulating the criteria which is necessary in achieving physically accurate solution of the equation, thus unify the deduction of heuristic selections of N for solving the contaminated fluids problem that leads to less pre-computation time. Note that inappropriate pair of Pe and N results in numerical oscillation [2]. The work presented in this paper follows the line initiated in Abdullah [2,3]'s studies for defining the sequence of both low Peclet numbers Pe and grid numbers N.

Various numerical methods for solving SCDE are by now well formulated and many useful schemes can be found such as finite differences, finite elements, spectral procedures, and the method of lines [4-17]. For instance, well-known a priori error estimates for the discontinuous Galerkin approximation of convection-dominated equation solutions which carry over to the subspace of the discontinuous piecewise-quadratic space was summarized in Melanie *et al.,* [4]'s study, while in Hailiang *et al.,* [5]'s study, the approximation of high order alternating evolution was proposed.

In Li *et al.,* [6]'s study, a comparative study between two most popular Lattice Boltzmann (LB) models for the equations (i.e. those in two dimensions with five and nine discrete lattice velocities, respectively) was presented. Other variants include multiple-relaxation-time LB model for the axisymmetric, as well as isotropic and anisotropic diffusion processes whose both applicability and accuracies have been investigated by previous studies [7,8], respectively; for the latter case, a finite-difference LB model for nonlinear equations was proposed by Huili *et al.,* [9]. In the problem where no scalar or flux jump exists, a numerical scheme for dealing with curved interfaces with second-order spatial accuracy was introduced by Ze-Xi *et al.,* [10] in conjunction with the LB method.

In both studies [11,12], compact difference scheme for solving convection-dominated equations was considered; It was claimed by Jun *et al.,* [11] that the fourth-order scheme requires only 15 grid points, while in Haiwei *et al.,* [12]'s study, it was successfully proven that this scheme is computationally more efficient than the standard second-order central difference scheme.

Introduction to a Schwarz waveform relaxation algorithm was introduced by Martin [13] for the convection-dominated equations that converge without overlap of the subdomains.

Recent methods include those to solve nonlinear fractional convection-dominated equations, as homotopy analysis transform and homotopy perturbation Sumudu transform methods whose reliability and efficiency were clearly demonstrated Jagdey *et al.,* [14], and that based on the operational matrices of shifted Jacobi polynomials of high accuracy [15].

The choice of suitable computational grid to discretize the governing partial differential equations (e.g. by means of polynomial fitting, Taylor series expansion and compact scheme to obtain approximations to the derivatives of the variables with respect to the coordinates) is necessary at the onset of numerical modelling of the scalar convection-dominated problems as in some studies [4-21]. It is worth to note here that the variable values at locations other than the defined grid nodes can also be determined by interpolation. Another important aspect is the method to solve the discretized algebraic equations. The solution is obtained via either direct [22-24] or iterative [25-28] methods.

In the following section, the SCDE is discretized on uniform grids, where the expansion factor $r_e = 1$. A Fourier series is utilized to model the spatial error resulting from insufficient grid number. The criterion for predicting φ profile without non-physical oscillation is then formulated.

Notwithstanding the fact that scalar convection-dominated flows have been widely studied among researchers, the contribution of the Peclet number Pe and the grid number N in predicting non-oscillatory solutions remains unclear. It is important to study such contribution in order to increase the efficiency in selecting the computational domain grid, and in eliminating some heuristic parts of the scalar concentration estimate. This research aims at formulating the condition to avoid spurious oscillatory solutions, which depends on both Pe and N.

2. Methodology

2.1 Discretization and Solution of The Governing Equation

The starting point is the SCDE in differential form as given by Eq. (6);

$$\partial_x(\rho u\varphi) - \partial_x(\epsilon\partial_x\varphi) = 1$$

Defining the boundary conditions as

$$\varphi(0) = \varphi(1) = 0 \tag{7}$$

Here we define the Peclet number Pe as

$$Pe = \frac{\rho uL}{\epsilon}$$

The influence of the Peclet number Pe on the diffusivity coefficient ϵ can be found in Yuezhen *et al.,* [26]'s study. The profiles for different ranges of Pe are illustrated in Figure 1.

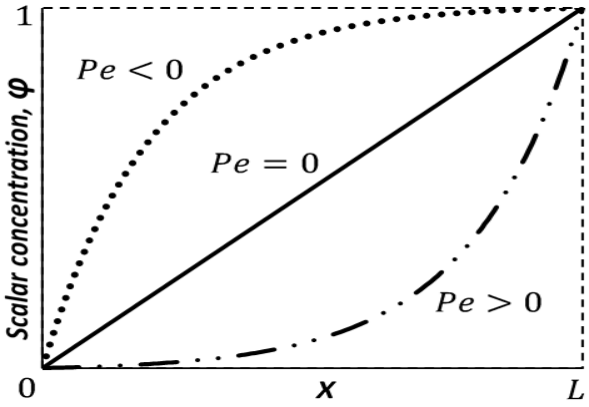

Fig. 1. Boundary conditions and solution profiles as a function of the Peclet number

A grid covers the corresponding solution domain. We define the independent variables x whose domain is discretized. The interval $x = [0,1]$ is subdivided into $(N-1)/h$ subintervals where N and h are integers. The nodes are defined by

$$x_{i+1} = x_i + r_e x_i$$

where $1 \leq i \leq (N-1)$, $i \in \mathbb{Z}$, and r_e is the grid expansion factor. Clearly $\sum x_{i+1} = 1$. The grid is shown in Figure 2.

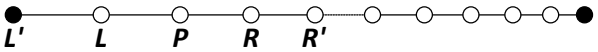

Fig. 2. Computational molecules

At each node, the governing equation is approximated by replacing the partial derivatives with nodal values. The result is an algebraic SCDE per node, in which the variables at that and immediate nodes appear as unknowns. The system of equations is expressed by

$$C_P \varphi_P + \sum_m C_m \varphi_m = Q_p, \tag{8}$$

where *P* signifies the nodes at which the equations are assigned and m index runs over the immediate nodes. The corresponding matrix C in Eq. (8) has non-zero terms only on its main diagonal (represented by C_{ii}) and the diagonals immediately above and below it (represented by C_R and C_L, respectively). The matrix elements are stored as three $n \times n$ array. Using the three-point computational molecules, Eq. (8) becomes

$$C_P \varphi_P + C_R \varphi_{i+1} + C_L \varphi_{i-1} = Q_P \tag{9}$$

Since the scalar convection-dominated differential equation is linear, then the approximation contains only linear terms, and the numerical solution will not require linearization. The central difference scheme (CDS) is used to discretize the diffusion term, both for the outer derivative

$$-[\partial_x(\epsilon \partial_x \varphi)]_i \approx \frac{(\epsilon \partial_x \varphi)_{i+\frac{1}{2}} - (\epsilon \partial_x \varphi)_{i-\frac{1}{2}}}{\frac{1}{2}(x_{i-1} - x_{i+1})} \tag{10}$$

and the inner derivative

$$\left.\begin{aligned}(\epsilon\partial_x\varphi)_{i+\frac{1}{2}} &\approx \epsilon\frac{\varphi_{i+1}-\varphi_i}{x_{i+1}-x_i}\\ -(\epsilon\partial_x\varphi)_{i-\frac{1}{2}} &\approx \epsilon\frac{\varphi_i-\varphi_{i-1}}{x_{i-1}-x_i}\end{aligned}\right\} \tag{11}$$

as well as the convection term

$$-[\partial_x(\rho u\varphi)]_i \approx \rho u\frac{\varphi_{i+1}-\varphi_{i-1}}{x_{i-1}-x_{i+1}} \tag{12}$$

The contributions of the diffusion and convection terms to the coefficients of the algebraic Eq. (8) are therefore

$$\begin{aligned}C_R &= C_R^{conv}+C_R^{diff}\\ &= \frac{\rho u}{x_{i+1}-x_{i-1}}-\frac{2\epsilon}{(x_{i+1}-x_{i-1})(x_{i+1}-x_i)};\\ C_L &= C_L^{conv}+C_L^{diff}\\ &= -\frac{\rho u}{x_{i+1}-x_{i-1}}-\frac{2\epsilon}{(x_{i+1}-x_{i-1})(x_i-x_{i-1})};\\ C_P &= C_P^{conv}+C_P^{diff}\\ &= -\left(C_R^{diff}+C_L^{diff}\right)\end{aligned}$$

Tridiagonal matrix algorithm is applied for solving linear system of the algebraic Eq. (9). We set

$$\rho = 1.0,\ u = 1.0,\ r_e = 1 \tag{13}$$

Note that the minimization of grid number might lead to spurious oscillation, i.e. the solution is nonphysical as depicted in Figure 3.

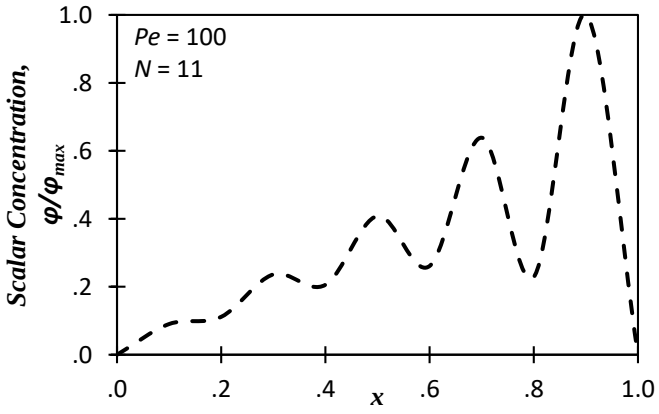

Fig. 3. Nonphysical behaviour of scalar concentration profile φ due to the insufficient grid number in computational domain

2.2 Sequences of The Peclet Numbers and The Grid Numbers

The range of low Peclet numbers Pe of interest is $[0,100]$. The mathematical relationship between Pe and grid numbers N is represented by a set of pairs $(Pe_i,\ N_j)$.
We define a sequence of Pe_i by

$$\begin{aligned} &Pe_i, \\ &Pe_{i+1} = Pe_i(p), \\ &Pe_{i+2} = Pe_{i+1}(p), \\ &Pe_{i+3} = Pe_{i+2}(p), \\ &Pe_n = Pe_{n-1}(p), \end{aligned} \tag{14}$$

where the constants $i,\ p \in \mathbb{Z}^+$. Next, defining a sequence of N by

$$\begin{aligned} &N_j\ , \\ &N_{j+1} = floor\left(\frac{N_j+1}{q}\right)\ , \\ &N_{j+2} = floor\left(\frac{N_{j+1}+1}{q}\right), \\ &N_{j+3} = floor\left(\frac{N_{j+2}+1}{q}\right), \\ &N_m = floor\left(\frac{N_{m-1}+1}{q}\right), \end{aligned} \tag{15}$$

where the constants $j,\ q \in \mathbb{Z}^+$. Let

$$i = j = 1, n = m = 6, Pe_1 = 3.125, N_1 = 81, \text{and } p = q = 2, \tag{16}$$

such that the sequence in Eq. (14) and Eq. (15) become

$$3.125, 6.25, 12.5, 25, 50, 100$$

and

$$81,\ 41,\ 21,\ 11,\ 6,\ 3$$

respectively. All 36 possible pairs $(Pe,\ N)$based on the elements in these sequences are considered as test cases, following the line used in previous studies [2,3,29,30].

2.3 Spatial Error Growth Model

Substituting Eq. (10), Eq. (11), and Eq. (12) into Eq. (6);

$$\frac{\varphi_{i+1}-\varphi_{i-1}}{2\varepsilon} = \frac{\varphi_{i+1}-2\varphi_i+\varphi_{i-1}}{\Delta x} + \frac{\Delta x}{\varepsilon} \tag{17}$$

The spatial error is defined as

$$\gamma = N - E, \tag{18}$$

where N and E are finite accuracy numerical solution from a real computer and exact solution of difference equation, respectively. Note that the numerical solution N satisfies the difference Eq. (17). A Fourier series model can be used to analytically represent the random variation of γ with respect to space;

$$\gamma(x) = \sum_l e^{\alpha x} e^{ik_l x},\ l = 1,2,3..., \tag{19}$$

where $e^{\alpha x}$ is the amplification factor, k_l is the wave number, and α is a constant. Lets $e^{\alpha x}$ in Eq. (19) be proportional to x when numerical oscillation occurs as represented in Figure 3. Thus it is sufficient to consider only the growth of $e^{\alpha x}$. Direct substitution of $e^{\alpha x}$into the finite difference Eq. (17) gives

$$\frac{e^{\alpha(x+\Delta x)} - e^{\alpha(x-\Delta x)}}{2\epsilon} = \frac{e^{\alpha(x+\Delta x)} - 2e^{\alpha x} + e^{\alpha(x-\Delta x)}}{\Delta x} \tag{20}$$

Divide Eq. (20) by $e^{\alpha x}$, we have

$$\frac{e^{\alpha\Delta x} - e^{-\alpha\Delta x}}{2\epsilon} = \frac{e^{\alpha\Delta x} - 2 + e^{-\alpha\Delta x}}{\Delta x}$$

which, after some rearrangement, becomes

$$e^{\alpha\Delta x} = \frac{e^{-\alpha\Delta x}(\Delta x + 2\epsilon) - 4\epsilon}{\Delta x - 2\epsilon}$$

If $e^{\alpha x}$ presumably grows with respect to x, then $\frac{e^{\alpha(x+\Delta x)}}{e^{\alpha x}} > 1$, or simply $e^{\alpha\Delta x} > 1$. Therefore, in order to have a non-growing error amplification, the criterion

$$\frac{e^{-\alpha\Delta x}(\Delta x + 2\epsilon) - 4\epsilon}{\Delta x - 2\epsilon} \leq 1 \tag{21}$$

must be fulfilled.

3. Result and Discussion

Rewriting Eq. (21) in terms of Pe and N;

$$\frac{e^{-\frac{\alpha}{N-1}}\left(\frac{1}{N-1} + \frac{2}{Pe}\right) - \frac{4}{Pe}}{\frac{1}{N-1} - \frac{2}{Pe}} \leq 1 \tag{22}$$

We define

$$G = \frac{e^{-\frac{\alpha}{N-1}}\left(\frac{1}{N-1} + \frac{2}{Pe}\right) - \frac{4}{Pe}}{\frac{1}{N-1} - \frac{2}{Pe}}$$

Thus Eq. (22) becomes

$$G \leq 1 \tag{23}$$

The criterion in Eq. (23) was checked against all 36 possible pairs (Pe_i, N_j) based on sequences Eq. (14) and Eq. (15). The output is given in Table 1. For $Pe = 3.125$, all grid numbers in sequence Eq. (15) are appropriate in achieving physically accurate non-oscillatory solutions. This is indicated by G being less than or equal to 1. The appropriate range of N shrinks by one element each time the next Pe in sequence Eq. (14) is considered.

The values of G tabulated in Table 1 were verified by plotting the concentration φ which are numerically calculated for Pe against N as shown in Figure 4 and 5. It is confirmed now that in any case where $G > 1$, the numerical oscillations appear, and the amplitudes grow with respect to x. The only exception is φ profile at $(Pe, N) = (6.25,3)$ in Figure 4 and 5 which appear to be non-oscillating despite $G > 1$ as shown in Table 1. This will be briefly explained in the next section.

It is interesting to note that the numerical oscillations which appear in shaded plots in Figure 4 and 5 begin with a kink. These kinks are highlighted further in Figure 6 for better visual understanding.

Table 1
Range of grid numbers N that fulfils to the criterion in Eq. (23) where $\alpha = -0.1$. The shaded cells indicate cases where $G > 1$

Pe = 3.125		*Pe* = 6.25		*Pe* = 12.5		*Pe* = 25		*Pe* = 50		*Pe* = 100	
N	*G*	*N*	*G*	*N*	*G*	*N*	*G*	*N*	*G*	*N*	*G*
81		81		81		81		81	≤ 1	81	≤ 1
41		41		41	≤ 1	41	≤ 1	41		41	
21	≤ 1	21	≤ 1	21		21		21		21	
11		11		11		11		11	> 1	11	> 1
6		6		6	> 1	6	> 1	6		6	
3		3	> 1	3		3		3		3	

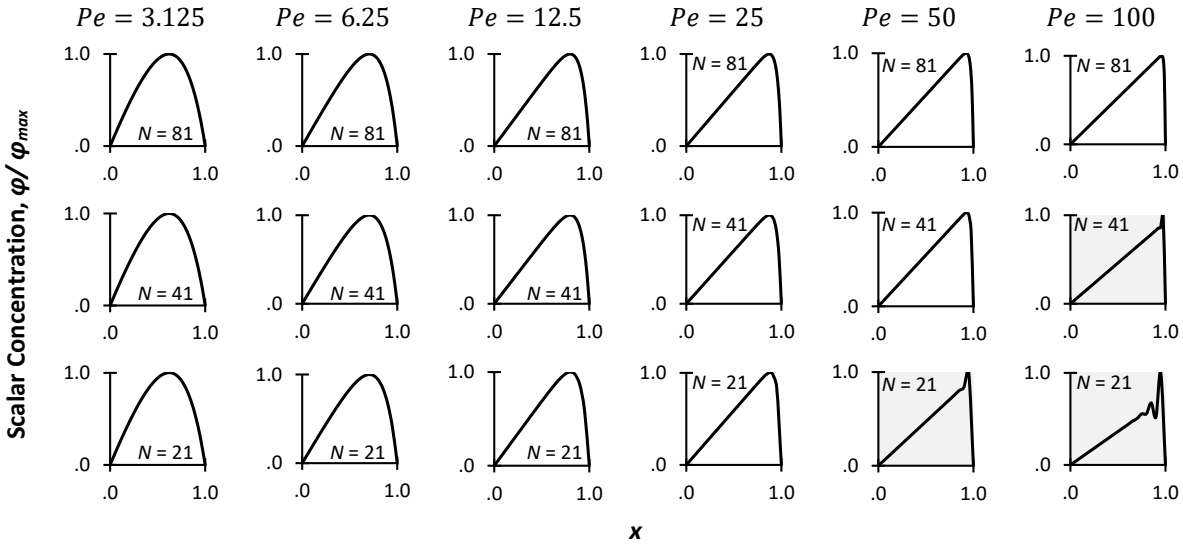

Fig. 4. Concentration profile φ/φ_{max} at Pe as in sequence Eq. (14) and $N = 81,41,21$. The shaded plots indicate cases where the numerical oscillations appear

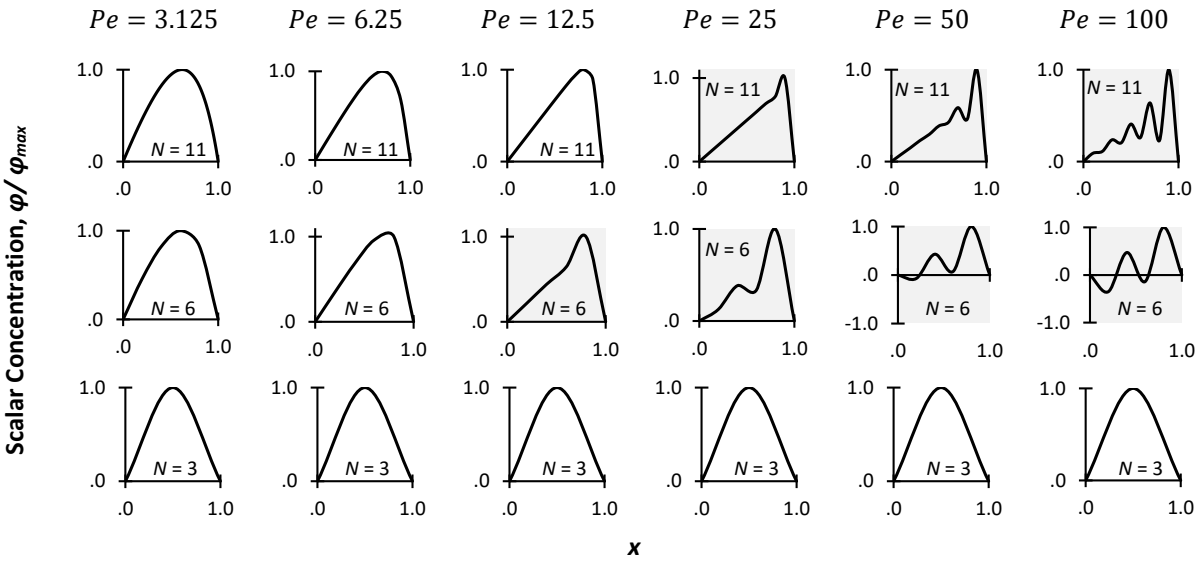

Fig. 5. Concentration profile φ/φ_{max} at Pe as in sequence Eq. (14) and $N = 11,6,3$. The shaded plots indicate cases where the numerical oscillations appear

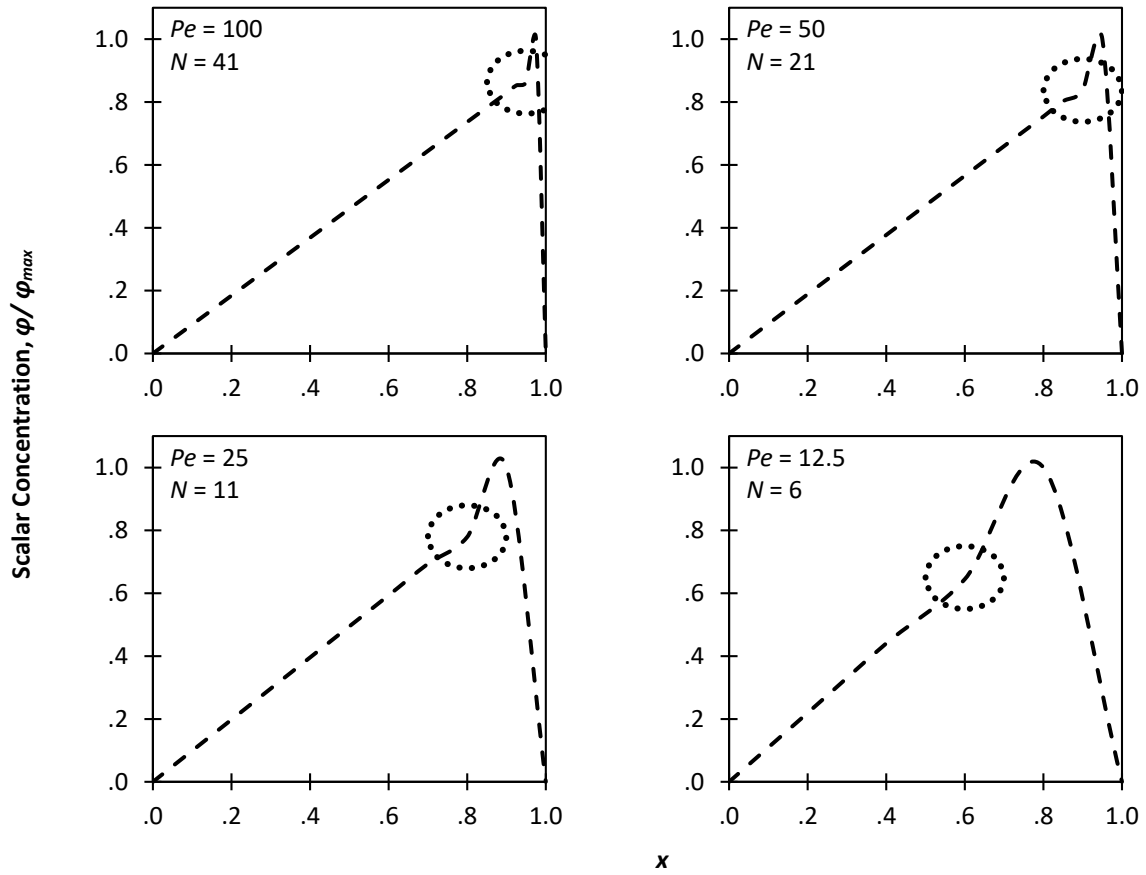

Fig. 6. Concentration profile φ/φ_{max} with clearer kinks which mark the beginning of the spurious oscillations at next Pe sequence. The kinks are marked by the circles

4. Conclusions

A condition to avoid numerical oscillation in the solution of scalar convection-dominated equations, SCDE, with source, s_φ, has been devised. The condition represents a qualitative guideline

that improves our understanding on the contribution of pair $(Pe,\ N)$to the oscillation, where Pe and N are Peclet number and grid number, respectively. The condition also gives the nominal values of N below which non-physical solutions occur. This sheds light on the possibility of a more general framework for the selection of grid type in computational fluid dynamics, the relationship between the flow parameter/s and the grid quality, as well as the influence of $(Pe,\ N)$ on various numerical error patterns.

It is found that the condition is able to capture the presence of kinks which mark the beginning of the oscillations. It is this capability that explains the anomaly involving the φ profile at $(Pe, N) = (6.25,3)$ in Figure 4 where there is no sign of oscillation despite $G > 1$; Even though the oscillations are preceded by a kink, it is impossible to capture the latter in a curve of three points (i.e. $N = 3$). Thus no oscillation can be captured in such profile.

Acknowledgement
The author would like to thank Universiti Tun Hussein Onn Malaysia (UTHM) and Ministry of Education of Malaysia (MoE) for the research facilities.

References

[1] Ferziger, Joel H., Milovan Perić, and Robert L. Street. "Finite difference methods." In *Computational methods for fluid dynamics*, pp. 41-79. Springer, Cham, 2020. https://doi.org/10.1007/978-3-319-99693-6_3
[2] Abdullah, Aslam. "Mathematical relationship between grid and low Peclet numbers for the solution of convection-diffusion equation." *ARPN J. Eng. Appl. Sci* 13, no. 9 (2018): 3182-3187.
[3] Abdullah, Aslam. "Obtaining grid number for the shooting method solution of convection-diffusion equation." *International Journal of Mechanical Engineering, & Technology (IJMET)* 9, no. 5 (2018): 916-924.
[4] Bittl, Melanie, Dmitri Kuzmin, and Roland Becker. "The CG1–DG2 method for convection–diffusion equations in 2D." *Journal of Computational and Applied Mathematics* 270 (2014): 21-31. https://doi.org/10.1016/j.cam.2014.03.008
[5] Liu, Hailiang, and Michael Pollack. "Alternating evolution discontinuous Galerkin methods for convection–diffusion equations." *Journal of Computational Physics* 307 (2016): 574-592. https://doi.org/10.1016/j.jcp.2015.12.017
[6] Li, Like, Renwei Mei, and James F. Klausner. "Lattice Boltzmann models for the convection-diffusion equation: D2Q5 vs D2Q9." *International Journal of Heat and Mass Transfer* 108 (2017): 41-62. https://doi.org/10.1016/j.ijheatmasstransfer.2016.11.092
[7] Li, Like, Renwei Mei, and James F. Klausner. "Multiple-relaxation-time lattice Boltzmann model for the axisymmetric convection diffusion equation." *International Journal of Heat and Mass Transfer* 67 (2013): 338-351. https://doi.org/10.1016/j.ijheatmasstransfer.2013.08.039
[8] Hu, Yang, Decai Li, Shi Shu, and Xiaodong Niu. "Lattice Boltzmann flux scheme for the convection–diffusion equation and its applications." *Computers & Mathematics with Applications* 72, no. 1 (2016): 48-63. https://doi.org/10.1016/j.camwa.2016.04.032
[9] Wang, Huili, Baochang Shi, Hong Liang, and Zhenhua Chai. "Finite-difference lattice Boltzmann model for nonlinear convection-diffusion equations." *Applied Mathematics and Computation* 309 (2017): 334-349. https://doi.org/10.1016/j.amc.2017.04.015
[10] Hu, Ze-Xi, Juntao Huang, Wei-Xi Huang, and Gui-Xiang Cui. "Second-order curved interface treatments of the lattice Boltzmann method for convection-diffusion equations with conjugate interfacial conditions." *Computers & Fluids* 144 (2017): 60-73. https://doi.org/10.1016/j.compfluid.2016.12.003
[11] Zhang, Jun, Lixin Ge, and Jules Kouatchou. "A two colorable fourth-order compact difference scheme and parallel iterative solution of the 3D convection diffusion equation." *Mathematics and Computers in simulation* 54, no. 1-3 (2000): 65-80. https://doi.org/10.1016/S0378-4754(00)00205-6
[12] Sun, Haiwei, Ning Kang, Jun Zhang, and Eric S. Carlson. "A fourth-order compact difference scheme on face centered cubic grids with multigrid method for solving 2D convection diffusion equation." *Mathematics and computers in Simulation* 63, no. 6 (2003): 651-661.

https://doi.org/10.1016/S0378-4754(03)00095-8
[13] Martin, Véronique. "An optimized Schwarz waveform relaxation method for the unsteady convection diffusion equation in two dimensions." *Applied Numerical Mathematics* 52, no. 4 (2005): 401-428. https://doi.org/10.1016/j.apnum.2004.08.022
[14] Singh, Jagdev, Ram Swroop, and Devendra Kumar. "A computational approach for fractional convection-diffusion equation via integral transforms." *Ain Shams Engineering Journal* 9, no. 4 (2018): 1019-1028. https://doi.org/10.1016/j.asej.2016.04.014
[15] Behroozifar, Mahmoud, and Afsane Sazmand. "An approximate solution based on Jacobi polynomials for time-fractional convection–diffusion equation." *Applied Mathematics and Computation* 296 (2017): 1-17. https://doi.org/10.1016/j.amc.2016.09.028
[16] Basha, M., and CS Nor Azwadi. "Numerical study on the effect of inclination angles on natural convection in entrance region using regularised lattice Boltzmann BGK." *Journal of Advanced Research in Fluid Mechanics and Thermal Sciences* 10, no. 1 (2015): 11-26.
[17] Sidik, Nor Azwadi Che, and Siti Aisyah Razali. "Various speed ratios of two-sided lid-driven cavity flow using lattice Boltzmann method." *Journal of Advanced Research in Fluid Mechanics and Thermal Sciences* 1, no. 1 (2014): 11-18.
[18] Tian, Zhen F., and P. X. Yu. "A high-order exponential scheme for solving 1D unsteady convection–diffusion equations." *Journal of computational and applied mathematics* 235, no. 8 (2011): 2477-2491. https://doi.org/10.1016/j.cam.2010.11.001
[19] Mittal, R. C., and R. K. Jain. "Redefined cubic B-splines collocation method for solving convection–diffusion equations." *Applied Mathematical Modelling* 36, no. 11 (2012): 5555-5573. https://doi.org/10.1016/j.apm.2012.01.009
[20] Cao, Huai-Huo, Li-Bin Liu, Yong Zhang, and Sheng-mao Fu. "A fourth-order method of the convection–diffusion equations with Neumann boundary conditions." *Applied Mathematics and Computation* 217, no. 22 (2011): 9133-9141. https://doi.org/10.1016/j.amc.2011.03.141
[21] Shukla, H. S., and Mohammad Tamsir. "An exponential cubic B-spline algorithm for multi-dimensional convection-diffusion equations." *Alexandria engineering journal* 57, no. 3 (2018): 1999-2006. https://doi.org/10.1016/j.aej.2017.04.011
[22] Biringen, Sedat. "A note on the numerical stability of the convection-diffusion equation." *Journal of Computational and Applied Mathematics* 7, no. 1 (1981): 17-20. https://doi.org/10.1016/0771-050X(81)90002-4
[23] Zhai, Shuying, Xinlong Feng, and Yinnian He. "An unconditionally stable compact ADI method for three-dimensional time-fractional convection–diffusion equation." *Journal of Computational Physics* 269 (2014): 138-155. https://doi.org/10.1016/j.jcp.2014.03.020
[24] Zhou, Zhongguo, and Dong Liang. "The mass-preserving and modified-upwind splitting DDM scheme for time-dependent convection–diffusion equations." *Journal of Computational and Applied Mathematics* 317 (2017): 247-273. https://doi.org/10.1016/j.cam.2016.10.031
[25] Ge, Lixin, and Jun Zhang. "High accuracy iterative solution of convection diffusion equation with boundary layers on nonuniform grids." *Journal of Computational Physics* 171, no. 2 (2001): 560-578. https://doi.org/10.1006/jcph.2001.6794
[26] Ma, Yuezhen, and Yongbin Ge. "A high order finite difference method with Richardsonextrapolation for 3D convection diffusion equation." *Applied Mathematics and Computation* 215, no. 9 (2010): 3408-3417. https://doi.org/10.1016/j.amc.2009.10.035
[27] Mohamed, S. A., N. A. Mohamed, AF Abdel Gawad, and M. S. Matbuly. "A modified diffusion coefficient technique for the convection diffusion equation." *Applied Mathematics and Computation* 219, no. 17 (2013): 9317-9330. https://doi.org/10.1016/j.amc.2013.03.014
[28] Boret, Saúl E. Buitrago. "Integrated framework for solving the convection diffusion equation on 2D Quad mesh relying on internal boundaries." *Computers & Mathematics with Applications* 74, no. 1 (2017): 218-228. https://doi.org/10.1016/j.camwa.2017.03.001
[29] Abdullah, Aslam. "Formulation of low Peclet number based grid expansion factor for the solution of convection-diffusion equation." *Eng. Technol. Appl. Sci. Res* 8 (2018): 2680-2684.
[30] Abdullah, Aslam. "Grid expansion factor for the shooting method solution of convection-diffusion equation." *ARPN J. Eng. Appl. Sci* 14, no. 7 (2006):1370-1376.